

Analyst

Accepted Manuscript



This is an *Accepted Manuscript*, which has been through the Royal Society of Chemistry peer review process and has been accepted for publication.

Accepted Manuscripts are published online shortly after acceptance, before technical editing, formatting and proof reading. Using this free service, authors can make their results available to the community, in citable form, before we publish the edited article. We will replace this *Accepted Manuscript* with the edited and formatted *Advance Article* as soon as it is available.

You can find more information about *Accepted Manuscripts* in the [Information for Authors](#).

Please note that technical editing may introduce minor changes to the text and/or graphics, which may alter content. The journal's standard [Terms & Conditions](#) and the [Ethical guidelines](#) still apply. In no event shall the Royal Society of Chemistry be held responsible for any errors or omissions in this *Accepted Manuscript* or any consequences arising from the use of any information it contains.

PAPER

Single-molecule force-spectroscopic study on stabilization of G-quadruplex DNA by telomerase inhibitor

Ryoto Funayama,^a Yoshio Nakahara,^a Shinpei Kado,^a Mutsuo Tanaka^b and Keiichi Kimura^{*a}

Received 00th January 2012,
Accepted 00th January 2012

DOI: 10.1039/x0xx00000x

www.rsc.org/

Single-molecule force spectroscopy was carried out using AFM force measurements for the purpose of the direct observation of the stabilization of G-quadruplex DNA by a telomerase inhibitor, which is 5,10,15,20-tetrakis(*N*-methylpyridinium-4-yl)porphyrin tetrakis(*p*-toluenesulfonate) (TMPyP). In AFM force measurements, we used an AFM tip and an Au substrate modified chemically with terminal-biotinylated telomere DNA and streptavidin, respectively. The telomere DNA was fully stretched by the AFM tip based on the bridge formation between the AFM tip and the Au substrate through the streptavidin-biotin interaction. The force-extension curves, which reflected the stretching of a single DNA molecule, were distinguished from all of the curves, judging from the rupture force and the contour length. The selected curves were analyzed using a worm-like chain model, and one of the fitting parameters, persistence length (l_p), was used as an index for the stabilization of the G-quadruplex structure. Consequently, the l_p value was significantly increased by the addition of TMPyP under the experimental conditions where the G-quadruplex structure could be formed. On the other hand, the value was hardly changed by the addition of TMPyP under the conditions except the above. Furthermore, the methodology developed and demonstrated in this work was applied to evaluate the stabilization of G-quadruplex DNA by other telomerase inhibitors such as ethidium bromide and *p*-xylene-bis(*N*-pyridinium bromide).

Introduction

Telomeres are the specialized ends of linear chromosomes and extend beyond the DNA duplex to form a single-stranded guanine-rich overhang.¹⁻³ They are deeply involved in a variety of functions such as meiotic chromosome segregation, chromatin silencing, and protecting the ends of the chromosomes from degradation or end-to-end fusion.⁴ In most organisms, telomeres are composed of simple repetitive sequences and in human they consist of several thousand repeats of the sequence 5'-TTAGGG repeats.^{1,2} The enzyme telomerase plays a crucial role to add the repeat sequences onto the telomere end in order to maintenance the proper length for the successive rounds of cell division.^{5,6} However, telomerase is abnormally activated in most malignant or cancer cells, and this may result in the continuous elongation of telomeres and the generation of immortal cells.⁷⁻⁹ Therefore, the inhibition of telomerase activity has attracted much attention as a new approach for cancer therapy.¹⁰⁻¹²

The single-stranded overhangs of human telomeres are known to form intramolecular four-stranded DNA structures, which are called as G-quadruplex (Fig. 1A), under specific conditions.¹³ The G-quadruplex effectively inhibits the telomerase activity by changing the single-stranded DNA

structure into an inactive conformation (Fig. 1B) that is no longer recognized by telomerase.¹⁴

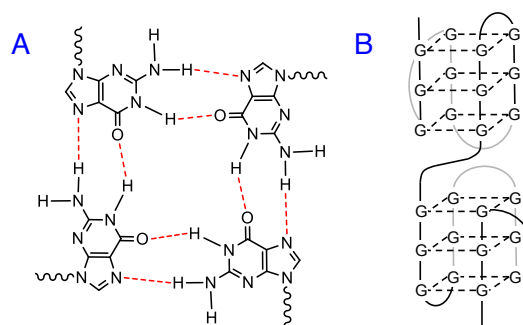
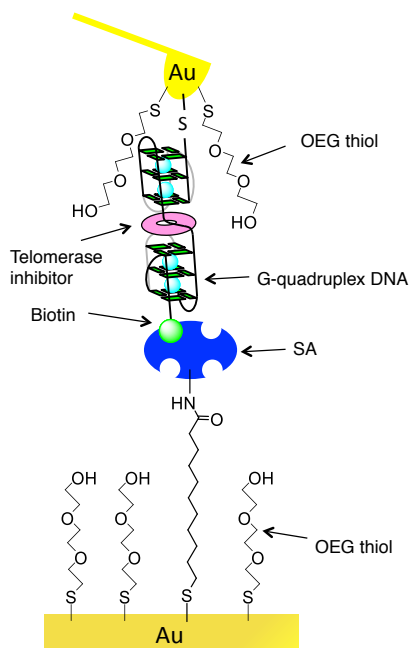


Fig. 1 (A) G-quadruplex. (B) DNA conformation based on G-quadruplex formation.

Also, it is well known that the G-quadruplex structure is stabilized by several ligands and that this event significantly improves the inhibitory effect of telomerase activity. These telomerase inhibitors include acridine derivatives,¹⁵ telomestatin,¹⁶ cyclic heterohelicene derivatives,¹⁷ and square-

1 planar nickel(II) complexes.¹⁸ Among them, a cationic
 2 porphyrin, 5,10,15,20-tetrakis(*N*-methylpyridinium-4-
 3 yl)porphyrin tetrakis(*p*-toluenesulfonate) (TMPyP), shows the
 4 strong telomerase inhibitory effect due to the electrostatic
 5 interaction and intercalation effect.¹⁹ Though a variety of
 6 techniques to analyze telomerase activity have been developed
 7 so far,²⁰⁻²² there has been little analytical method to evaluate the
 8 stabilization of the G-quadruplex structure by telomerase
 9 inhibitors directly.^{23,24}

10 In recent years, single-molecule force spectroscopy (SMFS)
 11 based on atomic force microscopy (AFM) has been
 12 demonstrated as a powerful tool to investigate a variety of
 13 biological phenomenon such as protein folding,²⁵ protein-
 14 ligand interactions,²⁶⁻²⁸ and DNA base-pairing.^{29,30} According
 15 to these studies, SMFS can potentially provide unique insights
 16 into the structure, function, and stability of target compounds
 17 on the single molecule level. The recent development of
 18 theoretical analysis has enabled reliable evaluation for the
 19 elastic behavior of the single polymer chain. For example, the
 20 mechanical and hydration properties of elastin-like
 21 polypeptides (ELP) were investigated by SMFS on the single
 22 molecule level.³¹ In that study, force-extension curves were
 23 analyzed using a freely jointed chain model and one of the
 24 fitting parameters, Kuhn segment length that reflects the
 25 flexibility of polymer chain, varied based on the hydrophobic
 26 hydration behavior of ELP. In addition, the mechanical
 27 properties of poly(vinyl alcohol) and poly(vinyl acetate) were
 28 examined using SMFS under different solvent conditions.³²
 29 Therein, force-extension curves were analyzed using a worm-
 30 like chain model and one of the fitting parameters, persistence
 31 length that reflects the flexibility of polymer chain, varied
 32 based on the conformation of the polymers. Thus, the fitting
 33 parameters obtained by SMFS can be an index for analyzing the
 34 structure and conformation of polymers.



37
38
39
40
41
42
43
44
45
46
47
48
49
50
51
52
53
54
55
56
57
58
59
60
Fig. 2 Schematic diagram of our AFM-based SMFS study.

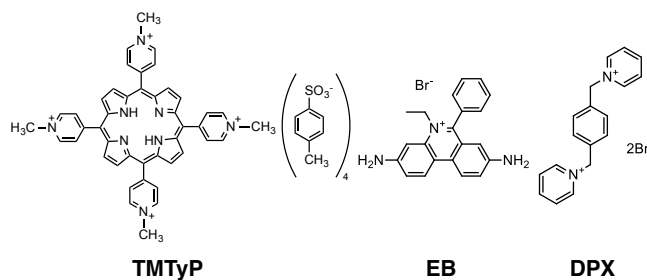


Fig. 3 Chemical structures of telomerase inhibitors used in this study.

Herein, we aimed at the direct observation of the stabilization of G-quadruplex DNA by telomerase inhibitors using AFM-based SMFS. We used an AFM tip and an Au substrate modified chemically with terminal-biotinylated telomere DNA and streptavidin (SA), respectively. The intermolecular bonding between SA and biotin is considered as the strongest receptor-ligand interaction found in nature.^{33,34} This intermolecular bonding has been used for the bridge formation between the AFM tip and the Au substrate in the previous SMFS study.³⁵ Fig. 2 outlines the strategy of this SMFS study, wherein the telomere DNA is thiolated at its 5' position end for covalently anchoring to a gold-coated AFM tip and biotinylated at the 3' position end for binding with the SA-modified substrate. In this experimental system, when the AFM tip contacts the substrate, the telomere DNA on the AFM tip is immobilized to the substrate through the SA-biotin interaction. When the AFM tip is retracted from the substrate, a rupture force originating from the cleavage of the SA-biotin interaction, which is distinguishable from that originating from non-bonding interactions, can be observed. As a telomerase inhibitor, TMPyP was selected here because it is commercially available and it shows the strong inhibition effect based on its four positive charges and flatness originating from the porphyrin skeleton.¹⁹ The force-extension curves, which reflected the stretching of a single DNA molecule, were distinguished from all of the curves, judging from the rupture force and the contour length. The selected curves were analyzed using a worm-like chain model, one of the fitting parameters, persistence length, was used as an index for the stabilization of the G-quadruplex structure by TMPyP. Furthermore, the stabilization of TMPyP was semi-quantitatively compared with that of ethidium bromide (EB), which is known to be a derivative of acridine showing a comparatively weak ability to stabilize the G-quadruplex structure,²³ and *p*-xylene-bis(*N*-pyridinium bromide) (DPX), which is a structural analogue of TMPyP. The chemical structures of telomerase inhibitors used here are shown in Fig. 3. Although AFM-based SMFS studies for intra- and intermolecular interactions of G-quadruplex with the target protein³⁵ and the stability of G-quadruplex DNA itself³⁶ have been reported previously, any report about the stabilization of G-quadruplex DNA by telomerase inhibitors has not been published yet, as far as we know.

Experimental section

Materials

The telomere DNA (5'-HS-CH₂CH₂CH₂CH₂CH₂CH₂-TTT(TTAGGG)₃TTAGGG(TTAGGG)₃TTAGGG-biotin-3'), which consists of a quadruplex dimer formed by two G-quadruplex repeats,¹⁷ was purchased from Invitrogen. Streptavidin (SA) from *Streptomyces avidinii* was purchased from Wako Pure Chemical Industries. 11-Mercaptoundecanoic acid (MUA), ethidium bromide (EB), and *p*-xylene-bis(*N*-pyridinium bromide) (DPX) were purchased from Sigma-Aldrich Japan. *N*-Hydroxysuccinimide (NHS) was obtained from Nacalai Tesuque. 1-Ethyl-3-(3-dimethylaminopropyl)carbodiimide hydrochloride (water-soluble carbodiimide; WSC), 5,10,15,20-tetrakis(*N*-methylpyridinium-4-yl)porphyrin tetrakis(*p*-toluenesulfonate) (TMPyP), and cacodylic acid were purchased from Tokyo Kasei Kogyo. All chemicals were used without further purification.

2-{2-[2-(2-Mercaptoethoxy)ethoxy]ethoxy}ethanol (OEG thiol) was synthesized according to the previous paper.³⁷ Deionized water (resistivity: 18 MΩ cm) was prepared using a Milli-Q system.

Circular dichroism (CD) measurements

The CD measurements were performed at room temperature using a spectropolarimeter (J-725, JASCO) for identifying the G-quadruplex formation of the telomere DNA used in this study. The concentration of the telomere DNA was set at 20 μM in 2.0 mM cacodylate buffer (pH 7.0) containing 50 mM KCl, 100 mM KCl, or 50 mM LiCl. Each measurement was recorded from 220 to 340 nm in a 1 cm-path length quartz cell at a scanning rate of 20 nm min⁻¹.

Chemical modification

The AFM tip and the Au substrate used for AFM force measurements were prepared by the chemical modifications with thiol compounds via a thiol-Au bond (Fig. 4). The V-shaped AFM cantilevers were commercially available: Si₃N₄ type coated with Au/Cr on both sides ($k = 0.02 \text{ N m}^{-1}$, OMCL-TR400PB-1, Olympus). Cantilevers were pretreated by immersing into a piranha solution (concentrated H₂SO₄/28% H₂O₂, 7/3, v/v) for 30 min for cleaning their surface (CAUTION: Piranha solution is extremely dangerous and should be handled with great care). The cantilevers were then thoroughly rinsed with ultra pure water. The cleaned cantilevers were immersed for 24 h into 2.0 mM cacodylate buffer (pH 7.0) containing 1.0 μM DNA. The DNA concentration was set at the very low concentration for one molecule to attach the AFM tip. After the cantilevers modified chemically with the telomere DNA were rinsed with 2.0 mM cacodylate buffer, they were immersed for 2 h into an aqueous solution containing 10 mM OEG thiol. The OEG thiol was introduced to decrease non-specific adhesion forces between the AFM tip and the Au substrate.^{38,39} After being rinsed with cacodylate buffer, they were dried with nitrogen gas before measurements.

Au-coated mica substrates were prepared by sputtering of gold (99.999%, Nilaco) using a JFC-1600 Auto Fine Coater (JEOL) onto a mica substrate prepared by fresh cleavage of a sheet of natural mica (Nilaco). The Au substrate was immersed

for 24 h into an ethanol solution containing 1.0 mM MUA and 10 mM OEG thiol at room temperature. The MUA was used to attach SA via the coupling reaction with amine.⁴⁰ After being rinsed with ethanol, the substrate was immersed for 30 min into an aqueous solution containing 100 mM WSC and 100 mM NHS at room temperature for the activation of terminal carboxyl group. After being rinsed with deionized water, the substrate was immersed for 2 h into 2.0 mM cacodylate buffer containing 0.10 mg mL⁻¹ SA. After being rinsed with cacodylate buffer, they were dried with nitrogen gas before measurements.

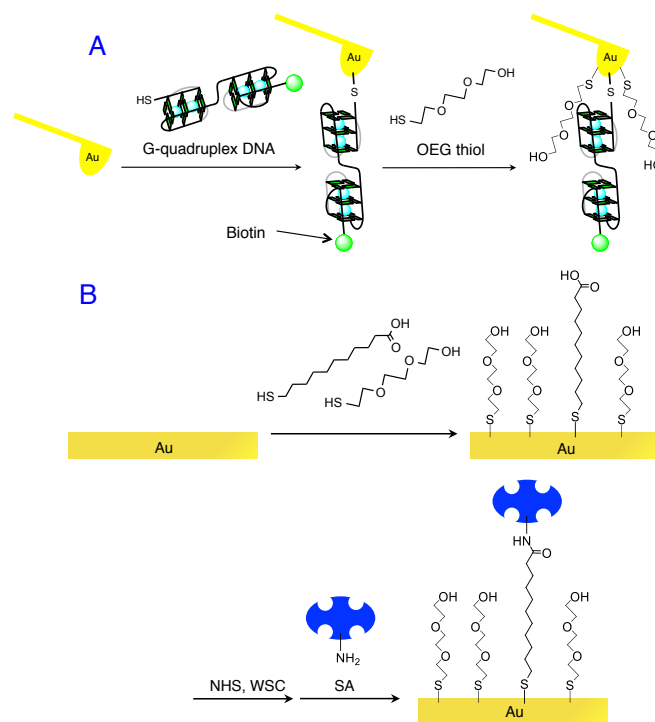


Fig. 4 Preparation of (A) AFM tip and (B) Au substrate modified chemically with terminal-biotinylated telomere DNA and SA, respectively.

X-ray photoelectron spectroscopy (XPS) measurements

The XPS apparatus (JPS-9010MC, JEOL) was used for identifying the chemical modification of SA on the Au substrate. The measurements were performed using Mg Kα X-ray, and the pressure in the ultrahigh vacuum chamber during measurements was lower than 10⁻⁹ torr. The accelerating voltage and emission current were maintained at 10 kV and 10 mA, respectively.

AFM force measurements

The AFM force measurements were carried out in 2.0 mM cacodylate buffer at room temperature (ca. 298 K) using a Nanoscope 3D MultiMode AFM with PicoForce (Veeco). The probe tip and the substrate were mounted on the apparatus using a liquid cell. The spring constants (typically 0.02 N m⁻¹) of the cantilever were always calibrated using the thermal tune method before each measurement. All force-distance curves were obtained in a contact mode using an AFM software of the manufacturers at a scan rate of 230 nm s⁻¹. Since a loading rate is the product of spring constant and scan rate, the loading rate was fixed at 4.6 nN s⁻¹ in this measurement system. The surface

delay, defined as the resting time after the tip touches the substrate surface, and the contact force were set at 5.0 s and 0.50 nN, respectively, to cause the bridge formation between the AFM tip and the Au substrate based on the SA-biotin interaction. The concentrations of TMPyP, EB, and DPX as the inhibitor were set at 1.0 μM , 1.0 μM , and 2.0 μM , respectively. The AFM force measurements were made more than 5,000 times for each experimental set, and the average observable probability for the stretching of the single DNA chain was 0.30% in total. The low observable probability may be due to the low introduction amount of the DNA on the tip, which enables us to analyze the stretching behavior of the DNA at a single molecule level. The obtained force-distance curves were converted to force-extension curves. Then, a theoretical model for polymer extension, worm-like chain (WLC) model, was used in order to obtain the characteristic fitting parameters. The calculations were repeated until the parameter converged. When the parameter did not converge, the curves were excluded from the analysis.

Results and discussion

Identification of G-quadruplex formation by CD measurements

The CD spectroscopy was used to verify the G-quadruplex formation of the telomere DNA used in this study. The previous reports have demonstrated that K^+ induced the G-quadruplex formation by diminishing the electrostatic repulsion between phosphate groups⁴¹ and that Li^+ induced the dissociation of the G-quadruplex structure.⁴² Fig. 5 shows the CD spectra of 20 μM DNA in 2.0 mM cacodylate buffer (pH 7.0) containing 50 mM KCl, 100 mM KCl, or 50 mM LiCl. In the cases containing KCl, the CD spectra showed a positive band around 290 nm and a negative band around 240 nm, which was the characteristic CD signature of a nonparallel G-quadruplex structure.⁴³ On the other hand, the characteristic peaks originating from the G-quadruplex structure were not observed in the case containing LiCl. As a result, we can tell that the telomere DNA can form the G-quadruplex structure in 2.0 mM cacodylate buffer (pH 7.0) containing KCl. As the CD spectra were almost the same between both cases containing 50 mM KCl and 100 mM KCl, it was found that 50 mM KCl was enough large in quantity to form the G-quadruplex structure.

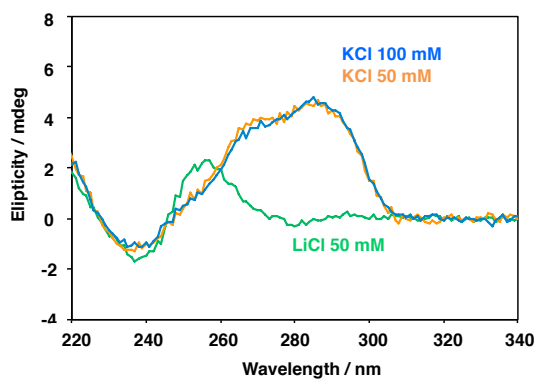


Fig. 5 CD spectra of telomere DNA in 2.0 mM cacodylate buffer (pH 7.0) containing 50 mM KCl, 100 mM KCl, or 50 mM LiCl.

Identification of chemical modification by XPS measurements

The XPS measurements were employed to confirm the presence of SA on the Au substrate. Fig. 6 shows the XPS spectra of the Au substrates before and after the chemical modification of SA. Before the chemical modification, only carbon, oxygen, and sulfur signals originated from MUA and OEG thiol were observed. After the chemical modification, a new nitrogen signal was observed in addition to these signals. The nitrogen signal may be originated from amino acids of SA. Therefore, it was experimentally verified that the chemical modification reaction of SA successfully proceeded on the Au substrate.

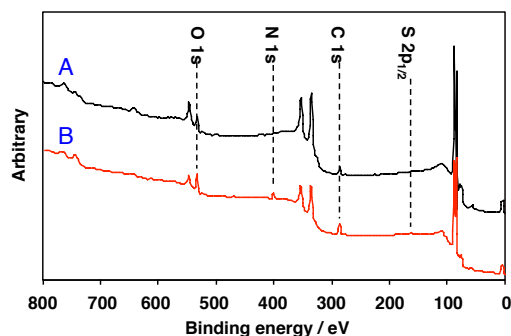


Fig. 6 XPS spectra of Au substrates (A) before and (B) after chemical modification of SA.

AFM force measurements

The AFM force measurements were carried out in 2.0 mM cacodylate buffer (pH 7.0) at room temperature using the AFM tip and the substrate modified chemically with the terminal-biotinylated telomere DNA and SA, respectively. It is generally known that the Au-S bond (typically 1.4 nN)⁴⁴ is at least 10 times stronger than the SA-biotin interaction. As the rupture force for the SA-biotin interaction is much larger than the breaking force of the G-quadruplex structure, which ranges from 23 to 60 pN,³⁶ the sequence of the rupture force should be G-quadruplex structure < SA-biotin interaction < Au-S bond.

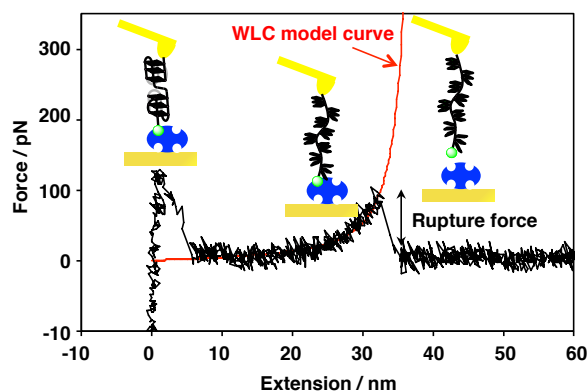


Fig. 7 Typical force-extension curve (black) in 2.0 mM cacodylate buffer (pH 7.0) containing 50 mM KCl and its theoretical curve (red) fitted based on WLC model.

The typical force-extension curve in 2.0 mM cacodylate buffer (pH 7.0) containing 50 mM KCl is shown in Fig. 7. The zero force and displacement points were defined as the force observed after a rupture point and the contact position between the tip and the substrate, respectively. In the course of the tip

retraction from the surface, the force-extension curve exhibited the deformational characteristics: a non-specific adhesion based on the contact between the tip and the substrate, a sharp rising force with increasing extension, followed by an abrupt dropping force upon the rupture between the tip and the substrate. We interpreted this retraction behavior as follows. When the tip modified with the terminal-biotinylated telomere DNA was in contact with the substrate modified with SA, the molecular bridge between the tip and the substrate formed through the SA-biotin interaction. Then, when the tip and the substrate were separated, a rupture force signal, which corresponds to the rupture of the weakest bond of the molecular bridge, appeared. Here, it was thought that the SA-biotin bond was cleaved upon the rupture between the tip and the substrate. In fact, such rupture forces were hardly observed in the presence of 10 mM biotin (data is not shown). This result suggested that the added biotin in the solution interfered the complexation of the biotin on the tip with SA on the substrate. As the SA-biotin interaction is much larger than the breaking of the G-quadruplex structure, the breaking is sure to occur before the rupture between the tip and the substrate. Therefore, the breaking of the G-quadruplex structure should be recorded in the force-extension curves.

Force curve selection and analysis using theoretical model

As has been reported by some researchers,⁴⁵ polymer stretching can be described by several theoretical models. Here, we used a theoretical model, worm-like chain (WLC) model,⁴⁶ to analyze the force-extension curves for the stretching of the telomere DNA. The WLC model describes a single polymer chain as a string of constant bending elasticity with a worm-like conformation. The following expression has been widely used to describe the force (F) as a function of chain extension (x).

$$F(x) = \frac{k_B T}{l_p} \left[\frac{1}{4} \left(1 - \frac{x}{L} \right)^{-2} + \frac{x}{L} - \frac{1}{4} \right]$$

where L represents the contour length of the polymer chain, k_B is the Boltzmann constant, T is the temperature, and l_p is the persistence length, indicating the rigidity/flexibility of the polymer chain. Based on the above-mentioned equation, curve fitting was conducted for the experimentally obtained force-extension curves to gain the characteristic fitting parameters of l_p and L .

Table 1 Experimental conditions and persistence length obtained by WLC model analysis

Entry	Metal salt ^a	Telomerase inhibitor ^b	Persistence length l_p / nm
1	KCl	None	0.231 ± 0.05 (n=26)
2	KCl	TMPyP	0.410 ± 0.07 (n=27)
3	LiCl	None	0.250 ± 0.02 (n=14)
4	LiCl	TMPyP	0.210 ± 0.06 (n=11)
5	KCl	EB	0.319 ± 0.03 (n=25)
6	KCl	DPX	0.223 ± 0.05 (n=12)

^a The concentration of the metal salt was 50 mM.

^b The concentration of TMPyP, EB, and DPX were 1.0 μM, 1.0 μM and 2.0 μM, respectively.

Fig. 7 also shows the theoretical curve fitted based on the WLC model. As the force curves, which seem to be originated

from the stretching of plural DNA chains, were not obviously fitted with the WLC model, they were excluded from the analysis. However, it is possibility that all the fitting curves do not always show the full stretching of the single DNA chain. Therefore, the following calibration was carried out. Here, we regarded the fitting curves with 25-40 nm of L and 90-150 nN of rupture force as the full stretching of the single DNA chain among all of the curves. This judge is based on the two reasons. One reason is that the total length of the DNA used in this study was estimated to be about 30 nm according to the reference, where contour length per base is assumed to be 0.56 nm in single-stranded DNA.⁴⁷ Another reason is that the intermolecular SA-biotin interaction was determined to 124.5 pN at a loading rate of about 3.0 nN s⁻¹ in the previous study.³⁵ The ranges of contour length and rupture force were enlarged to some extent because contour length and rupture force depend on the position of the DNA introduced on the tip and the loading rate in the measurements, respectively. Table 1 shows the experimental conditions and the l_p values obtained by the WLC model analysis. As these data were evaluated from the selected force curves, the l_p values can be discussed at a single-molecule level in the next section.

Effect of metal salt on G-quadruplex stabilization by TMPyP

The CD measurements made it clear that the G-quadruplex structure could be formed in the presence of KCl and that it could not in the presence of LiCl. Therefore, the stabilization of the G-quadruplex structure by TMPyP in the presence of KCl should be much larger than that in the presence of LiCl. Entries 1-4 in Table 1 show the l_p values before and after the addition of TMPyP under various experimental conditions. Totally, the l_p values of single-stranded DNA were relatively low, compared with those (about 4 nm) determined by the fluorescence method in the previous study.⁴⁸ The difference would be originated from the situation of DNA in the analytical methods. In this study, as DNA molecules are individually immobilized on the tip, they are unable to associate with each other, unlike in the solution. Therefore, most of DNA on the tip may exist in a random coil structure, which lowers l_p values.

As expected, entries 1 and 2 demonstrated that the l_p value was significantly increased by the addition of TMPyP in the presence of 50 mM KCl. The increase of the l_p value definitely means that the conformation of the polymer was changed from a relaxed structure to a more stretched structure. This phenomenon is due to the fact that the telomere DNA was stabilized by the interaction between the G-quadruplex structure and TMPyP. On the other hand, the increase of the l_p value was not observed by the addition of TMPyP in the presence of 50 mM LiCl (entries 3 and 4). The result was not also contradictory to our expectation because the telomere DNA does not have the strong interaction with TMPyP under the conditions where the G-quadruplex structure is not formed. The lower l_p values in the presence of LiCl may be attributed to the unstabilization of the G-quadruplex structure by Li⁺. In fact, the l_p value was similar to the length (0.15 nm) of C-C bonding. This result shows that the DNA behaves like a flexible random coil in the presence of LiCl. Consequently, it has been found that the increase of the l_p value can be closely related to the stabilization of the G-quadruplex structure. Interestingly, the l_p value in the presence of KCl was almost the same as that in the presence of LiCl under the conditions without TMPyP (entries 1 and 3) although the CD spectra were really different between the above-mentioned two conditions. Probably, the association force of the G-quadruplex structure would be not enough large

to change the mechanical property of the DNA under the conditions without any telomerase inhibitor.

Comparison among telomerase inhibitors

Up to date, a lot of ligands have been shown to exhibit anti-telomerase activity in vitro. These molecules are able to stabilize the G-quadruplex structure, as shown by spectroscopic measurements. However, there are little reports about quantitative comparison of stabilization among telomerase inhibitors because spectroscopic measurements require specific functional groups emitting a spectroscopic signal. In other words, only structural analogues are comparable in these analytical methods. In contrast, AFM force measurements do not limit measuring compounds. Therefore, the methodology developed and demonstrated in this work is suitable for quantitative analysis between telomerase inhibitors whose structures are different each other.

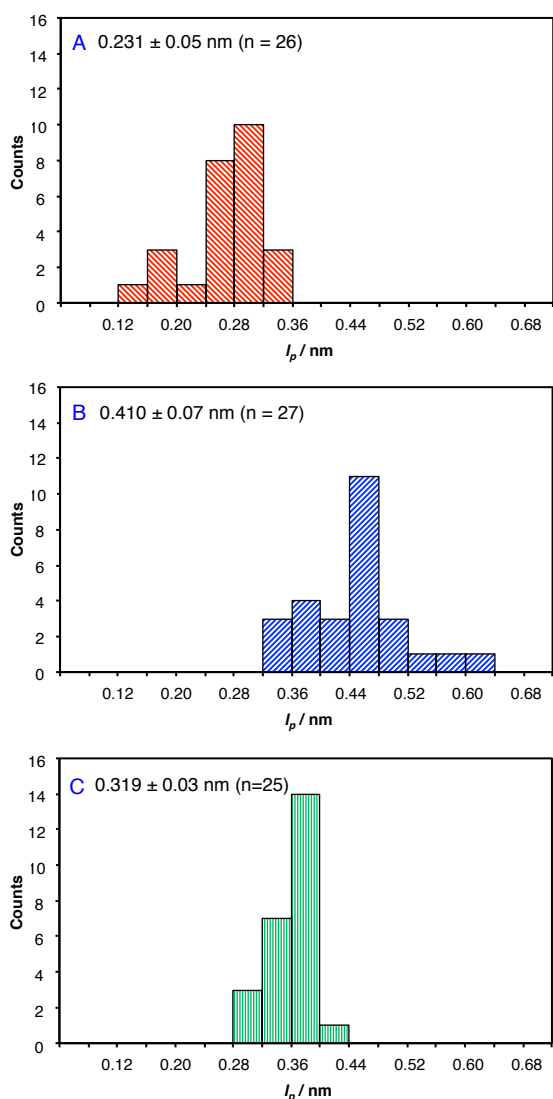


Fig. 8 Distributions of persistence length in 2.0 mM cacodylate buffer (pH 7.0) containing 50 mM KCl in the (A) absence and presence of (B) 1.0 μM TMPyP or (C) 1.0 μM EB.

Previously, EB, which is a derivative of acridine, has been reported to have a comparatively weak ability to stabilize the G-quadruplex structure.²³ Entry 5 in Table 1 shows the l_p value in the presence of 50 mM KCl after the addition of EB. The l_p value slightly increased by the addition of EB, but the variation amount was smaller than that by the addition of TMPyP. This result was consistent with our expectation because TMPyP is thought to show a considerably strong anti-telomerase activity among telomerase inhibitors.⁴⁹ Fig. 8 shows the distributions of the l_p values in 2.0 mM cacodylate buffer (pH 7.0) containing 50 mM KCl before and after the addition of TMPyP or EB. Here, the distributions were evaluated using Kruskal-Wallis test (analysis of variance without assumption of a Gaussian distribution). As a result, the difference between three histograms was considered statistically significant ($p < 0.05$).

Next, DPX, which is a structural analogue of TMPyP, was also investigated. As this compound has no porphyrin ring, it seems that DPX does not show an ability to intercalate between the G-quadruplex structures. In the SMFS measurement, the concentration of DPX was set at two times as much as that of TMPyP in order to unify the charge effects. According to entry 6 in Table 1, the l_p value was almost the same as that in the absence of any telomerase inhibitor (entry 1). Therefore, it is considered that DPX has no anti-telomerase activity. From our SMFS study, it is predicted that the sequence of the telomerase inhibitory effect should be $\text{TMPyP} > \text{EB} > \text{DPX} = \text{no stabilizer}$.

Conclusions

In summary, a new approach to investigate the stability of the G-quadruplex structure semi-quantitatively was developed using AFM-based SMFS in this study. As the increase in the persistence length of the telomere DNA was closely associated with the stabilization of the G-quadruplex structure, the persistence length obtained by our SMFS study could be a very useful index to evaluate the performance of telomerase inhibitors. An advantage over other techniques in this method is that we can measure at the very low concentrations of a telomere DNA and a telomerase inhibitor. In addition, this analytical method is suitable for quantitative analysis between telomerase inhibitors because AFM force measurements do not limit measuring compounds. Therefore, we expect that this analytical technique will provide important information in developing new type of telomerase inhibitors in the near future.

Notes and references

^aDepartment of Applied Chemistry, Faculty of Systems Engineering, Wakayama University, 930 Sakae-dani, Wakayama 640-8510, Japan, E-mail: kkimura@center.wakayama-u.ac.jp

^bNational Institute of Advanced Industrial Science and Technology, Central 5, 1-1-1 Higashi, Tsukuba, Ibaraki 305-8565, Japan

- 1 E. H. Blackburn, *Cell*, 1994, **77**, 621-623.
- 2 V. A. Zakian, *Science*, 1995, **270**, 1601-1607.
- 3 C. W. Greider, *Annu. Rev. Biochem.*, 1996, **65**, 337-365.
- 4 C. M. Counter, A. A. Avilion, C. E. LeFeuvre, N. G. Stewart, C. W. Greider, C. G. Harley and S. Bacchetti, *EMBO J.*, 1992, **11**, 1921-1929.
- 5 M. J. McEachern, A. Krauskopf and E. H. Blackburn, *Annu. Rev. Genet.*, 2000, **34**, 331-358.

- 1
2
3
4
5
6
7
8
9
10
11
12
13
14
15
16
17
18
19
20
21
22
23
24
25
26
27
28
29
30
31
32
33
34
35
36
37
38
39
40
41
42
43
44
45
46
47
48
49
50
51
52
53
54
55
56
57
58
59
60
- 6 N. W. Kim, M. A. Piatyszek, K. R. Prowse, C. B. Harley, M. D. West, P. L. Ho, G. M. Coviello, W. E. Wright, S. L. Weinrich and J. W. Shay, *Science*, 1994, **266**, 2011–2015.
- 7 G. B. Morin, *Cell*, 1989, **59**, 521–529.
- 8 S. B. Cohen, M. E. Graham, G. O. Lovrecz, N. Bache, P. J. Robinson and R. R. Reddel, *Science*, 2007, **315**, 1850–1853.
- 9 M. D. Stone, M. Mihalusova, C. M. O'Connor, R. Prathapam, K. Collins and X. Zhuang, *Nature*, 2007, **446**, 458–461.
- 10 T. R. Cech, *Angew. Chem., Int. Ed.*, 2000, **39**, 34–43.
- 11 E. M. Rezler, D. J. Bearss and L. H. Hurley, *Annu. Rev. Pharmacol. Toxicol.*, 2003, **43**, 359–379.
- 12 A. D. Cian, L. Lacroix, C. Douarre, N. T. Smaali, C. Trentesaux, J. Riou and J. L. Mergny, *Biochimie*, 2008, **90**, 131–155.
- 13 J.-L. Mergny and C. Helene, *Nat. Med.*, 1998, **4**, 1366–1367.
- 14 A. M. Zahler, J. R. Williamson, T. R. Cech and D. M. Prescott, *Nature*, 1991, **350**, 718–720.
- 15 F. Koepfel, J. F. Riou, A. Laoui, P. Mailliet, P. B. Arimondo, D. Labit, O. Petitgenet, C. Helene and J. L. Mergny, *Nucleic Acids Res.*, 2001, **29**, 1087–1096.
- 16 K. Shin-ya, K. Wierzbza, K. Matsuo, T. Ohtani, Y. Yamada, K. Furihata, Y. Hayakawa and H. Seto, *J. Am. Chem. Soc.*, 2001, **123**, 1262–1263.
- 17 K. Shinohara, Y. Sannohe, S. Kaieda, K. Tanaka, H. Osuga, H. Tahara, Y. Xu, T. Kawase, T. Bando and H. Sugiyama, *J. Am. Chem. Soc.*, 2010, **132**, 3778–3782.
- 18 J. E. Reed, A. A. Arnal, S. Neidle and R. Vilar, *J. Am. Chem. Soc.*, 2006, **128**, 5992–5993.
- 19 H. Han, D. R. Langley, A. Rangan and L. H. Hurley, *J. Am. Chem. Soc.*, 2001, **123**, 8902–8913.
- 20 S. Gelmini, A. Caldini, L. Becherini, S. Capaccioli, M. Pazzagli and C. Orlando, *Clin. Chem.*, 1998, **44**, 2133–2138.
- 21 C. Nemos, J. P. Remy-Martin, P. Adami, F. Arbez-Gindre, J. P. Schaal, M. Jouvenot and R. Delage-Mourroux, *Clin. Biochem.*, 2003, **36**, 621–628.
- 22 C. Ding, X. Li, Y. Ge and S. Zhang, *Anal. Chem.*, 2010, **82**, 2850–2855.
- 23 G. Breuzard, J.-M. Millot, J.-F. Riou and M. Manfait, *Anal. Chem.*, 2003, **75**, 4305–4311.
- 24 C. Wei, G. Jia, J. Yuan, Z. Feng and C. Li, *Biochemistry*, 2006, **45**, 6681–6691.
- 25 A. Borgia, P. M. Williams and J. Clarke, *Annu. Rev. Biochem.*, 2008, **77**, 101–125.
- 26 D. J. Müller and Y. F. Dufrene, *Nat. Nanotechnol.*, 2008, **3**, 261–269.
- 27 D. J. Müller, *Biochemistry*, 2008, **47**, 7986–7998.
- 28 K. C. Neuman and A. Nagy, *Nat. Methods*, 2008, **5**, 491–505.
- 29 L. H. Pope, M. C. Davies, C. A. Laughton, C. J. Roberts, S. J. B. Tendler and P. M. Williams, *Eur. Biophys. J.*, 2001, **30**, 53–62.
- 30 M. Vander Wal, S. Kamper, J. Headley and K. Sinniah, *Langmuir*, 2006, **22**, 882–886.
- 31 A. Valiaev, D. W. Lim, S. Schmidler, R. L. Clark, A. Chilkoti and S. Zauscher, *J. Am. Chem. Soc.*, 2008, **130**, 10939–10946.
- 32 H. Li, W. Zhang, W. Xu and X. Zhang, *Macromolecules*, 2000, **33**, 465–469.
- 33 L. Chalet and F. J. Wolf, *Arch. Biochem. Biophys.*, 1964, **106**, 1–5.
- 34 N. M. Green, *Adv. Protein Chem.*, 1975, **29**, 85–133.
- 35 X.-Q. Zhao, J. Wu, J.-H. Liang, J.-W. Yan, Z. Zhu, C. J. Yang and B.-W. Mao, *J. Phys. Chem. B*, 2012, **116**, 11397–11404.
- 36 S. Lynch, H. Baker, S. G. Byker, D. Zhou and K. Sinniah, *Chem.-Eur. J.*, 2009, **15**, 8113–8116.
- 37 M. Tanaka, T. Sawaguchi, Y. Sato, K. Yoshioka and O. Niwa, *Tetrahedron Lett.*, 2009, **50**, 4092–4095.
- 38 K. L. Prime and G. M. Whitesides, *J. Am. Chem. Soc.*, 1993, **115**, 10714–10721.
- 39 C. Pale-Grosdemange, E. S. Simon, K. L. Prime and G. M. Whitesides, *J. Am. Chem. Soc.*, 1991, **113**, 12–20.
- 40 S. Inoue, Y. Nakahara, S. Kado, M. Tanaka and K. Kimura, *J. Surf. Anal.*, 2012, **18**, 164–173.
- 41 S. L. Jeremy, *Nucleic Acids Res.*, 1990, **18**, 6057–6060.
- 42 WO 2013/021536 A1, 2013.
- 43 J. Kypr, I. Kejnovská, D. Renčičuk and M. Vorličková, *Nucleic Acids Res.*, 2009, **37**, 1713–1725.
- 44 M. Grandbois, *Science*, 1999, **283**, 1727–1730.
- 45 M. I. Giannotti and G. J. Vancso, *ChemPhysChem*, 2007, **8**, 2290–2307.
- 46 A. Janshoff, M. Neitzert, Y. Oberdörfer and H. Fuchs, *Angew. Chem., Int. Ed.*, 2000, **39**, 3212–3237.
- 47 S. Iliafar, K. Wagner, S. Manohar, A. Jagota and D. Vezenov, *J. Phys. Chem. C*, 2012, **116**, 13896–13903.
- 48 B. Tinland, A. Pluen, J. Sturm and G. Weill, *Macromolecules*, 1997, **30**, 5763–5765.
- 49 M. Cavallari, A. Garbesi and R. D. Felice, *J. Phys. Chem. B*, 2009, **113**, 13152–13160.

Graphical abstract

The stabilization of G-quadruplex DNA by telomerase inhibitor was semi-quantitatively evaluated by AFM-based SMFS.

